DOI: 10.1002/adfm.201600179
Article type: Full Paper

Simple Salt-coordinated n-Type Nanocarbon Materials Stable in Air

Yoshiyuki Nonoguchi, Motohiro Nakano, Tomoko Murayama, Harutoshi Hagino, Shota Hama, Koji Miyazaki, Ryosuke Matsubara, Masakazu Nakamura, and Tsuyoshi Kawai**

Prof. Y. Nonoguchi, M. Nakano, T. Murayama, Prof. R. Matsubara, Prof. M. Nakamura, Prof. T. Kawai
Graduate School of Materials Science, Nara Institute of Science and Technology (NAIST)
Ikoma 630-0192, Japan
E-mail: nonoguchi@ms.naist.jp; tkawai@ms.naist.jp
Dr. H. Hagino, S. Hama, Prof. K. Miyazaki
Department of Mechanical and Control Engineering, Kyushu Institute of Technology
Kitakyushu 804-8550, Japan

Keywords: doping, stability, redox reactions, coordination, carbon nanotubes

Abstract

After more than three decades of molecular and carbon-based electronics, the creation of air- and thermally stable n-type materials remains a challenge in the development of future p/n junction devices such as solar cells and thermoelectric modules. Here we report a series of ordinary salts such as sodium chloride (NaCl), sodium hydroxide (NaOH) and potassium hydroxide (KOH) with crown ethers as new doping reagents for converting single-walled carbon nanotubes to stable n-type materials. Thermoelectric analyses revealed that these new n-type single-walled carbon nanotubes displayed remarkable air stability even at 100 ^{o}C for more than one month. Their thermoelectric properties with a dimensionless figure-of-merit (ZT) of 0.1 make these new n-type single-walled carbon nanotubes a most promising candidate for future n-type carbon-based thermoelectric materials.

1. Introduction

Nanocarbons including carbon nanotubes (CNTs) and graphenes are composed of robust sp^2-planer and quasi-planer carbon frameworks. They have been extensively studied for the development of future electronic and energy devices such as field-effect transistors (FETs),[1] solar cells,[2] and thermoelectrics.[3] With the aid of expanded sp^2 frameworks, nanocarbons have unique and advantageous properties such as high charge-carrier transport properties, relatively narrow bandgap energy, and mechanical toughness and flexibility.[4] Their low weight density, low toxicity, and ambient stability also make them promising for practical use.[5,6] The physicochemical and electronic properties of nanocarbons are predominantly modulated by the sign and the density of charge carriers and thus tuned by ionic and molecular doping along with the charge-injections.[7] Electrochemical doping/de-doping also alters the nature of charge carriers;[8] *i.e.* the Seebeck coefficient of CNTs from positive (p-type) to negative (n-type).[9] Precise doping can also be applied to tune the Dirac point in nanotube- and graphene-FETs.[10,11]

Meanwhile, the extremely-large surface area (>1000 m^2/g) of nanocarbons promotes efficient adsorption of various substances onto their sp^2 planes, such as organic molecules, ions and inorganic nanomaterials.[12] Most molecular and atomic adsorption onto nanocarbons relies on van der Waals interaction based on the π-π interaction and charge-transfer interaction with their π-electron systems. Electron spin resonance (ESR) and Raman spectra provide physicochemical insights into molecular chemisorption on nanocarbons accompanied by partial charge transfer interaction[13,14] Electron-accepting molecules induce a highly p-type doped state after electron uptake from nanocarbons. The injection of electrons from dopants to nanocarbons, conversely, compensates intrinsic positive charge carriers, and results in the generation of negatively charged major carriers that afford n-type nanocarbons.

Most as-prepared nanocarbons possess p-type majority charge carriers because of oxygen impurity. Since both p- and n-type materials are simultaneously required for some p/n

junction-based applications such as solar cells and thermoelectric devices, n-type nanocarbons have been extensively studied as a counter material of pristine p-type nanocarbons materials.[15] The chemical doping of metallic sodium and potassium typically form the n-type CNTs and graphenes.[16] Although their stability in ambient conditions are not high enough for practical applications, significant enhancement in the ESR spin density and conductivity, the n-type FET characteristics, and thermoelectric characterization with the negative Seebeck coefficients have been well established.[17-19] Improvement in ambient stability of n-doped CNTs has recently been studied using a cobalt-complex as a mild dopant for making CNTs n-type state.[20,21] Some nitrogen-containing organic molecules and polymers with much weaker electron-donating abilities have also been studied as n-type dopants for CNTs.[22-24] We have recently reported a series of phosphine-based dopants which are also highly efficient for affording n-type CNTs with improved stability.[25] However, considering the possible oxidation of these phosphine-, nitrogen- and Co(II)-based compounds, a quest for the stable and easy-to-handle dopants that can make nanocarbons stable in the n-type state is still highly challenging. In the scope of these previous reports on the n-type doping systems of CNTs, little attention has been paid to the chemical nature of charge compensating positive ions that should interact with the negatively charged n-type CNTs.

Here we report on stable and efficient n-type nanocarbon doping based on simple salts (**Figure 1a**): ordinary halide and hydroxide anions with tetraalkylammonium (R_4N^+) cations and cationic crown ether complexes with alkali ions (**Figure 1b**). We show a negative Seebeck coefficient of some typical nanocarbons such as CNTs, carbon fibers and graphenes after doping with them. The present n-type CNTs showed unprecedented long-term thermal stability at 150 °C in air, an essential requirement for thermoelectric powering applications.[26,27]

2. Results and Discussion

2.1. Stable n-type doping with ordinary salts

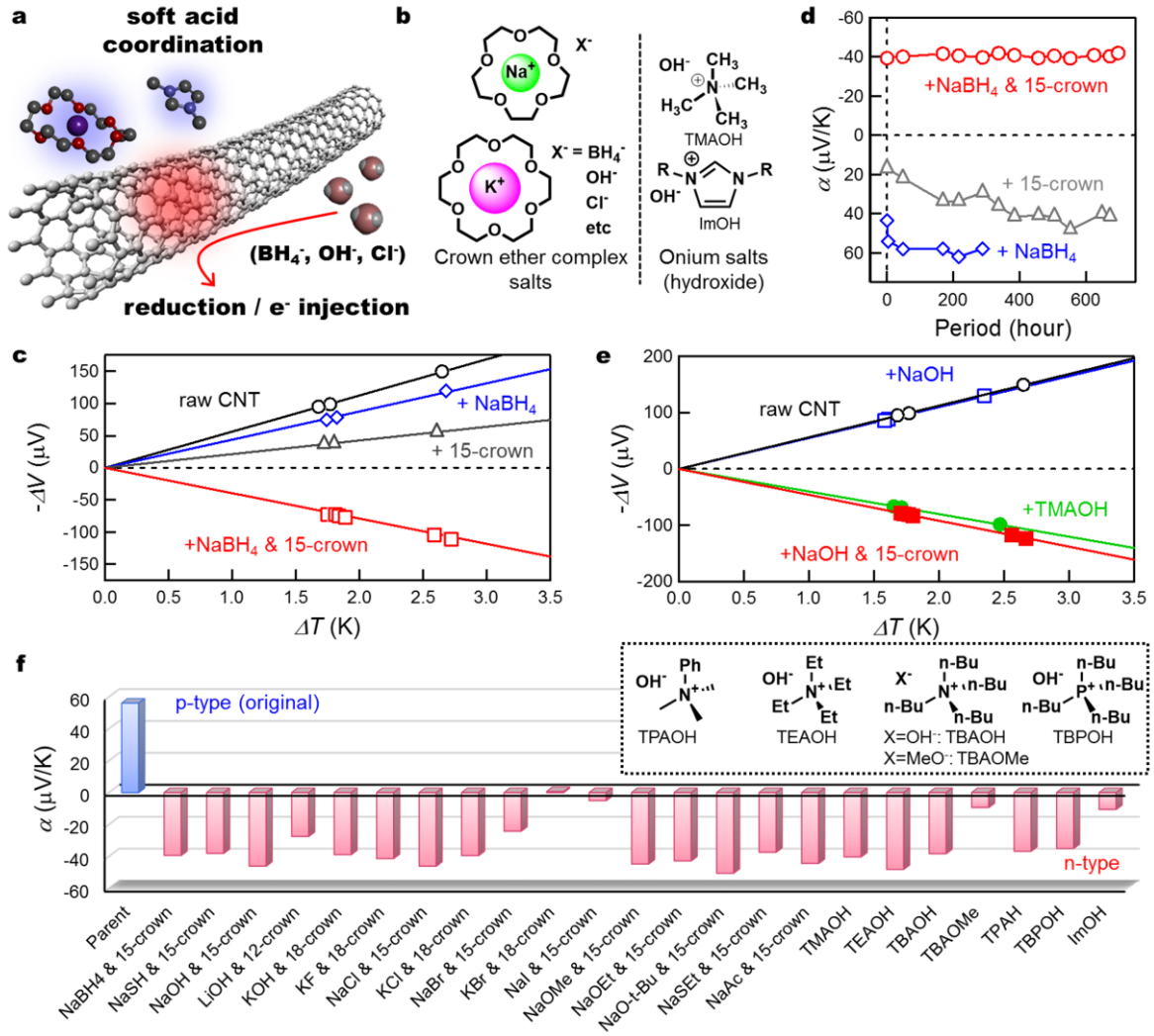

Figure 1. Salt-induced n-type doping. (a) Schematic concept of salt-induced n-type doping. (b) The typical n-type inducers in this work. (c) Thermovoltage of raw SWNT films, and their $NaBH_4$, 15-crown-5-ether, and both-treated films at 310 K. (d) Temporal changes of the Seebeck coefficient (α) of SWNT films treated solely with $NaBH_4$ or 15-crown-5-ether, and with both $NaBH_4$ and 15-crown-5-ether over a month under ambient conditions. (e) Thermovoltage of SWNT films reacted with TMAOH, NaOH, and NaOH/15-crown-5-ether along with raw SWNTs. (f) The Seebeck coefficient of SWNTs with typical 23 n-type inducers.

We first studied the n-type doping of single-walled carbon nanotubes (SWNTs, KH Chemicals HP-grade, denoted as KH-CNTs for a specific use) with a typical reducing agent, sodium borohydride ($NaBH_4$). In **Figure 1c**, voltage difference is plotted as a function of temperature difference between both ends of sample films (See Supplementary Information). The Seebeck coefficient (α) is defined by its gradient (α=-ΔV/ΔK). The voltage difference of

raw SWNTs showed a positive slope, corresponding to the p-type characteristics (the black line, **Figure 1c**). We observed a slight decrease in the positive thermovoltage of SWNTs after a reaction with $NaBH_4$, ascribed to the chemical reduction of SWNTs and the compensation of intrinsic holes (the blue line, **Figure 1c**). This suppressed thermovoltage reverted to the original value in a day (the blue plots, **Figure 1d**). Similar faint doping and spontaneous de-doping also occurred when another reducing agent, sodium hydrosulfide (NaSH), was used (**Figure S1**).[28] Interestingly, using 15-crown-5-ether with $NaBH_4$ and NaSH, we obtained a clearly negative slope (α <0, the red line, **Figure 1c** and **1f**). This sign inversion indicates the conversion of original p-type SWNTs into their n-type forms. Surprisingly, they exhibited remarkable air-stability over 700 h under ambient conditions. Neither salts nor the crown ether solely led to such n-type forms (**Figure 1c**) and air stability (**Figure 1d**). These observations suggest that the Na^+-15-crown complexes play a crucial role in the n-type doping process of SWNTs and their stabilization.

Furthermore, the use of crown ether complexes are further advantageous for dopants showing much weaker reducing power. Sodium hydroxide (NaOH) was available for this purpose in combination with the crown ether. **Figure 1e** shows the successful sign inversion of thermovoltage from the raw p-type SWNTs to their n-type forms through the treatment of a mixture of NaOH and crown ether. Here we present more than thirty successful n-type doping systems based on crown ethers with a number of ordinary salts including NaCl and KCl (**Figure 1f**, **Table S1**), which are usually not recognized as reducing (electron-injecting) reagents.[29] The efficient n-type doping was also observed with onium hydroxides such as tetramethylammonium hydroxide (TMAOH, the green line in **Figure 1e**) and 1-butyl-3-methylimidazolium hydroxide (ImOH in **Figure 1f**). This n-type doping procedure is conventionally applicable for some other carbon allotropes such as multi-walled CNTs and graphenes (**Figure S2**).

The origin of n-type doping with these rather non-reactive salts can be explained regarding the complexation of crown ethers with the alkali-metal ions. Crown ethers form their stable metal-ion complexes ($[M\text{-crown}]^+ X^-$) with relatively high binding constants ($K > 10^3\ M^{-1}$ in methanol).[30]

$$MX + [crown] \rightleftharpoons [M\text{-crown}]^+ X^- \quad (1)$$

M = Li, Na, K, etc
X = OH, MeO, Cl, etc

Considering the enhanced nucleophilic reactivity of "naked" counter anions,[31] the electron donating ability of OH^- and other anions could be high enough to n-type dope SWNTs. Typically, OH^- is a weak one-electron reducing reagent via the $[OH^-]$/[OH radical anion] couple and converts to hydrogen peroxide via two-electron transfer.[32-35] This might lead to the conversion of SWNTs into their reduced form as follows;

$$SWNT + OH^- \longrightarrow [SWNT]^- + 1/2\ H_2O_2 \quad (2)$$

In general, the reduction power of OH^- is considered rather weak or negligible in most protic solvents because the hydroxide ions are effectively solvated and stabilized via hydrogen bonding.[35] OH^- can be more reactive in aprotic solvents, which could promote the partial reduction of SWNTs via equations (1) and (2). Electron spin resonance study showed a slight increase in carbon radicals after the doping treatment with NaOH/crown ethers (**Figure S3**), corresponding to the electron transfer from salts to SWNTs.

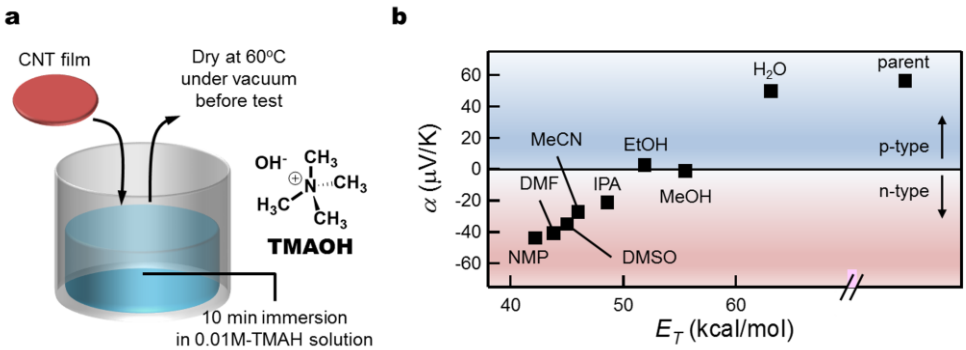

Figure 2. Solvent dependence of n-type doping. (a) An experimental procedure for the doping of SWNTs with TMAOH. (b) The Seebeck coefficient of TMAH-treated SWNT films as a function of the E_T value of solvents used. A saturated solution was used for isopropanol (IPA)

and acetonitrile (MeCN). Other solvents are indicated as abbreviations, e.g. water (H_2O), methanol (MeOH), ethanol (EtOH), dimethylsulfoxide (DMSO), dimethylformamide (DMF), and N-methylpyrrolidone (NMP). CNT films 84±4 μm in thickness and ~0.4 g/cm^3 in volumetric mass density were used. (TMAOH conc.= 0.01 mol/L, immersion period = 10 min)

It should be noted that the Seebeck coefficient is highly sensitive towards the nature of solvents used in the doping process. The solvent effect was studied by immersing thin CNT films into various solvents containing TMAOH as a typical dopant (**Figure 2a**). In **Figure 2b**, the Seebeck coefficient is plotted as a function of the solvent parameter E_T, the measure of the accepting nature of solvents used in the doping process.[36] With the E_T of solvents decreased, the negative Seebeck coefficient and the degree of n-type doping significantly increased. The relative stability of OH^- in various solvents, which depends on the E_T value, dominantly controls its electron injection tendency to SWNTs and their conversion to the n-doped state. The relative stability of delocalized negative charges on SWNTs will be sensitive to the accepting nature of solvents. Although the dielectric nature of the solvent might also play a substantial part, we here report a clearer tendency with the E_T value. This solvent effect also suggests that the "naked" OH^- ions could promote the formation of n-type SWNTs. It should be noted that the larger anions such as tetrafluoroborate (BF_4^-, ionic radius = 232 pm) and sulfate (SO_4^{2-}, ionic radius = 258 pm) did not serve as the n-type dopants for the SWNTs (**Figure S4**). In contrast, halide anions such as Cl^- and Br^- were efficient for the n-type doping of SWNTs, while it is possible to form neutral halogen molecules from Cl^- to Cl_2. A similar system based on the conversion of halide anions to halogen molecules has recently been reported for the reduction of silver ions (Ag^+) into metallic silver and nanoparticles.[37] We actually confirmed the reduction of Ag^+ ions to Ag nanoparticles with the salt-crown ether mixture, indicating its moderate reducing power (**Figure S5**).

2.2. Structural characterization

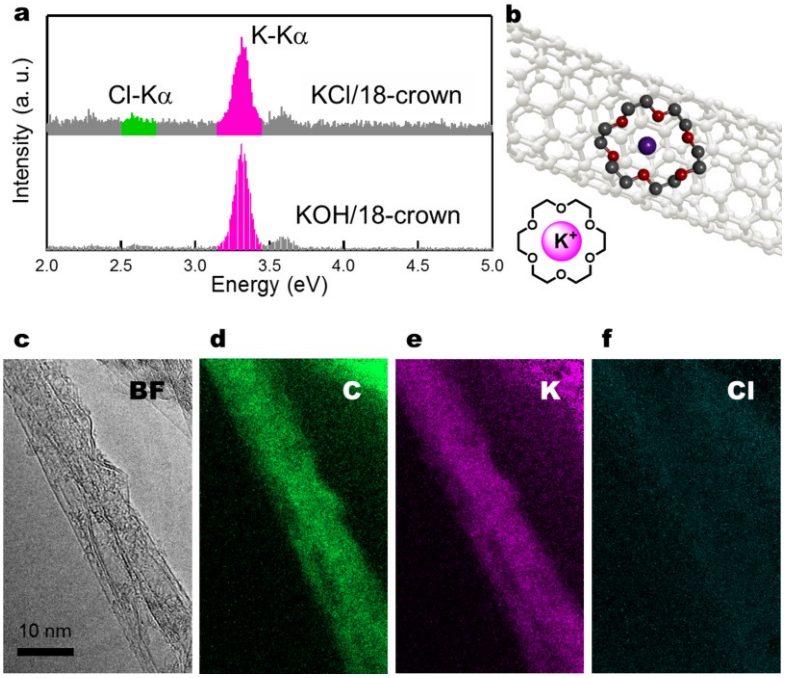

Figure 3. Molecular structures along doped SWNTs. (a) EDS of KOH/18-crown ether-treated, and KCl/18-crown ether-treated SWNTs. (b) A plausible product for salt-induced n-type doping of SWNTs. (c) bright field TEM and elemental mapping of (d) carbon (C), (e) potassium (K) and (f) chlorine (Cl) in the KCl/crown ether-treated n-type SWNTs. The mapping was performed by EELS.

We then carried out the microscopic elemental analysis of the n-type SWNTs. To specify the reactive species, we analyzed potassium cations (K^+) and chloride anions (Cl^-) in the n-type SWNTs. Energy dispersive X-ray spectroscopy (EDS, **Figure 3a**) revealed that the n-type film treated with KCl and 18-crown-6-ether contains a large amount of potassium but almost no chlorine. Elemental mapping experiments with electron energy-loss spectroscopy (EELS) further revealed that the nanotubes adsorbed K^+ ions and almost no halogen on their surface (**Figure 3c-f**). The positive charges of absorbed K^+ ions should be compensated by the negative charges on the SWNTs (**Figure 3b**), but not by the Cl^- ions. We thus believe that Cl^- ions were consumed and converted into Cl_2 gas or soluble byproducts such as Cl_3^-,[32] which were removed upon sample treatments with the pure solvents in advance to the measurements.

The n-type doping was also confirmed by the effective suppression of the typical optical absorption band of SWNTs, S_{11}-band corresponding to the band-gap optical transition (**Figure S6**). Raman spectroscopy provided the mechanistic insight for doping. By excitation

at 785 nm, it was hard to find a significant peak shift of a cooperative in-plane stretching mode of aromatic rings, called a G-band, at 1589 cm^{-1} between raw and salt-processed SWNTs (**Figure S7**). This might suggest that the n-type doping does not disturb C-C bond distortion unlike the well-known heavy n-type doping by alkali metals. The systematic, gradual suppression of the Raman band at less than 350 cm^{-1} (radial breathing mode, RBM) also supported the modulation of an sp^2 backbone with charge injection and/or the adsorption of ions (**Figure S7**).[7]

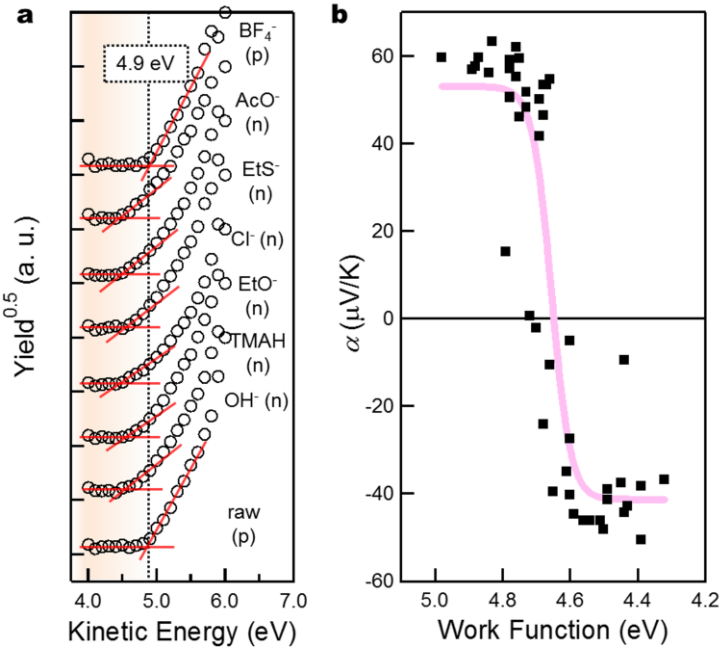

Figure 4. Characterization of the n-type doped SWNTs. (a) Ultraviolet photoelectron yield spectra of SWNT films (KH-CNTs) treated with TMAOH, or mixtures of typical sodium salts and 15-crown-5-ether to determine their work function. As typical sodium salts, hydroxide (OH^-), ethoxide (EtO^-), chloride (Cl^-), ethanethiolate (EtS^-), acetate (AcO^-), and tetrafluoroborate (BF_4^-) were examined. (b) The relationship between work function and the Seebeck coefficient (see Table S1 for raw data).

We examined the SWNTs' work function modulation upon n-type doping on the basis of ultraviolet photoelectron spectroscopy (UPS).[10, 25, 38] The onset energy in the UPS profile was roughly assigned to the work function and was shifted to lower energy upon n-type doping from those of raw films (**Figure 4a**). This upshift in the Fermi level indicates the electron injection from the dopant to the valence and conduction bands of SWNTs. The

Seebeck coefficients of KH-CNTs were measured after the treatment with various dopants and were correlated with the corresponding work functions in **Figure 4b**. The inversion of the Seebeck coefficient from the positive to the negative values was observed at the threshold of work function around 4.8 eV. The drop in the Seebeck coefficient was observed in a range of about 0.2 eV, which was comparable to the band gap of KH-CNTs (~0.3 eV). The Fermi level was roughly regarded as being controlled from the top of a valence band to the bottom of a conduction band by means of the present salt doping method. Since the Seebeck coefficient and the work function were both evaluated as the mean values over the SWNT ensembles, the intermediate values of the Seebeck coefficient in the transition region may be assigned to the averaged results over various SWNTs in the critical conditions.

2.3. Thermoelectric properties

Table 1. In-plane and through-plane thermoelectric properties at 310K.

sample[a)]	direction	σ [S/cm][c)]	α [μV/K][c)]	*power factor* [μW/mK^2]	κ [W/mK][d)]	*ZT (@310K)*
Parent film	in-plane	1.51×10^3	38	2.2×10^2	9.8±3.3	7×10^{-3}
	through-plane	65	89	52	0.13(9)±0.001	1×10^{-1}
Doped film[b)]	in-plane	2.05×10^3	-33	2.3×10^2	39±12	2×10^{-3}
	through-plane	69	-63	27	0.12(4)±0.001	7×10^{-2}

[a)] Parent films (buckypapers) were made from eDIPS-CNTs (Meijo Nanocarbon EC-P; [b)] These samples were prepared by treating the parent p-type films with KOH and 18-crown-6-ether in DMF; [c)] Four-point electrical conductivity and Seebeck coefficient at a through-plane direction was evaluated following the reported procedure[52]; [d)] Thermal diffusivity was measured with the periodic heating and Xenon flash methods for the in-plane and through-plane measuremants, respectively.

Considering the possibility of the n-type SWNTs for thermoelectrics,[21,26] the simultaneous improvement in electrical conductivity (σ) and the Seebeck coefficient (α) is important for the enhancement in the power factor ($\alpha^2\sigma$). At present and to our knowledge, no n-type carbon based-materials with power factors higher than 2×10^2 μW m^{-1}K^{-2} have been reported,[39-41] while corresponding p-type counterparts have been demonstrated.[42-49] In this

respect, we expanded our n-doping procedure to a highly conducting eDIPS-CNTs (Meijo Nanocarbon EC2.0). Here, their anisotropic thermoelectric performance was also evaluated and results are summarized in **Table 1**. An original buckypaper exhibited an in-plane conductivity of 1.5×10^3 S cm^{-1} with a Seebeck coefficient of 38 μV K^{-1}. It should be noted that the through-plane thermoelectric properties are quite different from those of the in-plane. The suppressed electrical and thermal conductivity with twice larger Seebeck coefficient provided a considerably large ZT value of 0.1.

After dipping into the stock solution of 0.1 mol/L KOH and 18-crown-6-ether and subsequent washing and drying, we obtained an n-type eDIPS-CNTs film with enhanced electrical conductivity (2.05×10^3 S cm^{-1}) and power factor (2.2×10^2 μW m^{-1}K^{-2}, in-plane, also see **Figure S8 and S9**, and **Table S2** for other SWNTs). This power factor is the highest among the n-type carbon-based thermoelectrics so far reported,[21,26] and comparable to those of most promising p-type organic materials.[41] We also studied thermal conductivity κ for efficient thermoelectric conversion. Using the periodic heating method in vacuo,[50] we obtained 39±12 W m^{-1}K^{-1} for in-plane thermal conductivity for the n-type eDIPS-CNTs film, four times larger than the original, 9.8±3.3 W m^{-1}K^{-1}.[51] The through-plane electrical conductivity of n-type eDIPS SWNTs (69 S cm^{-1}) was the thirtieth of the corresponding in-plane electrical conductivity (2.05×10^3 S cm^{-1}).[52] We obtained a through-plane ZT of 0.07 considering through-plane thermal conductivity of 0.124 W m^{-1}K^{-1} at 310 K. The ZT exceeded 0.1 above 150 ºC. Although this value is the highest among carbon-based n-type materials, exploration of its dramatic improvement is demanded for practical applications. Further fine tuning CNTs, e.g., in length, diameter and their distribution, seems necessary along with the doping procedures.

2.4. Thermal stability

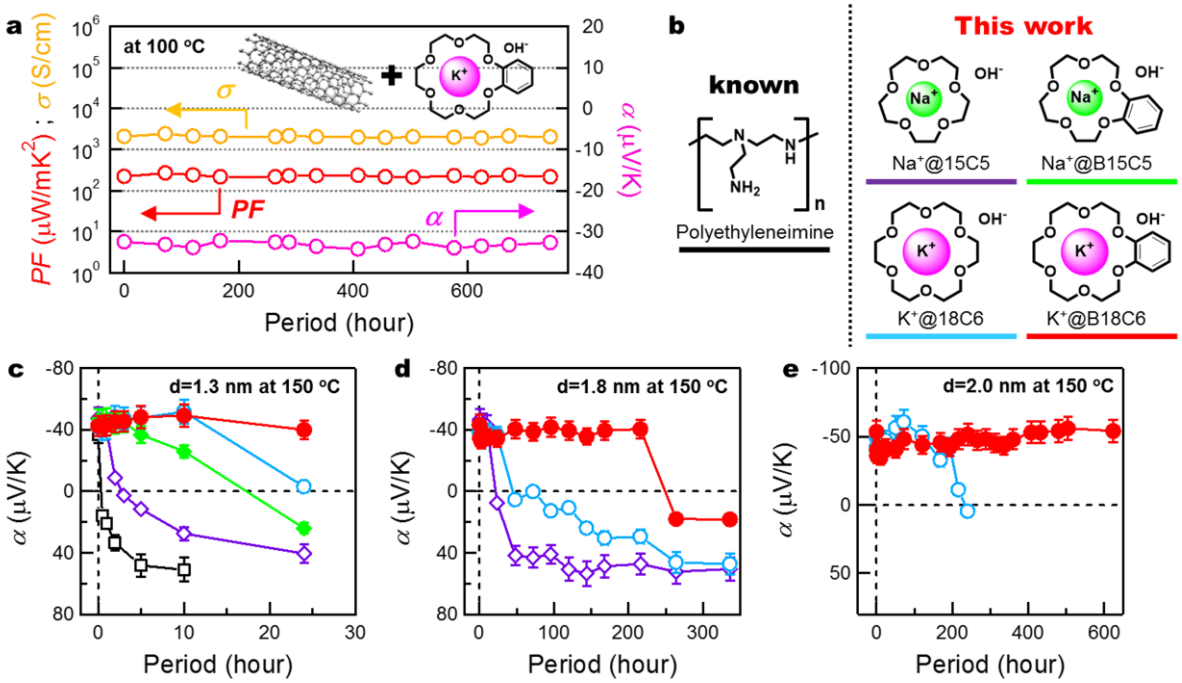

Figure 5. Thermal stability. (a) Temporal changes of the electrical conductivity (brown), the Seebeck coefficient (pink) and power factor (red) of n-type films derived from eDIPS-CNTs treated with KOH/benzo-18-crown ether at 100 °C. (b) Additives used in this study. Temporal changes of n-type films from (c) KH-CNTs 1.3±0.2 nm in diameter; (d) Tuball-CNTs 1.8±0.3 nm in diameter; (e) eDIPS-CNTs 2.0±0.7 nm in diameter at 150 °C. The color of plots in (c-e) corresponds to lines of (b) indicating molecular structures.

We further report a drastic improvement of thermal stability in the temperature range above 100 °C in air. For improved thermal stability, benzocrown ether derivatives were additionally studied as host dopants. With the combination of salts such as KOH and benzo-18-crown-6-ether, the SWNT films preserved the n-type characteristics at 100 °C at least for over 700 hours (> 1 month, **Figure 5a**). The salt-treated SWNTs exhibited considerable stability at 150 °C, while the Seebeck coefficient of polyethyleneimine (PEI)-wrapped SWNTs readily reverted from negative to positive in thirty minutes at the same temperature (**Figure 5c**). Although PEI has been recognized to form ambient-stable n-type nanocarbons, their stability doesn't seem high enough at the elevated temperature.[53] We obtained the most stable n-type SWNT films by using KOH and benzo-18-crown ether. These films showed exceptional stability in the negative Seebeck coefficient at 150 °C over 50 hours for KH-CNTs (**Figure 5c**), over 200 hours for other commercial SWNTs (OCSiAl Tuball) (**Figure 5d**), and

surprisingly over 600 hours for eDIPS-CNTs (**Figure 5e**). The Seebeck coefficient just after the sample was treated showed no marked dependence on the host dopant and thus the doping levels seems similar for all samples. The thermal transition to the positive Seebeck coefficient may thus be attributed to the auto-oxidation forming the p-type SWNTs. Thermogravimetry showed almost no mass change below 135 °C for the salt-treated SWNTs whereas the PEI-doped ones start to loss their gravity below 60 °C (**Figure S10**).

The significant thermal stability of the present n-type SWNTs can be explained tentatively in terms of the efficient stabilization of negatively charged SWNTs with the positive ions. The crown ether-based cations ($[M\text{-crown}]^+$) behave as soft Lewis acids and efficiently stabilize soft bases under the classical HSAB (hard and soft acids and bases) concept. In the solid state, charge polarizability could also control cation-anion charge balance. Reynolds and coworkers have reported that n-type poly(3,4-ethylenedioxythiophene) (PEDOT) derivatives are specifically stabilized by inserting larger cations such as tetranbutylammonium (TBA^+), indicating the contribution of HSAB theory.[54] Similarly, the negative charges on n-type SWNTs seem to be delocalized over many aromatic units, which can be efficiently stabilized by soft Lewis acids such as $[M\text{-crown}]^+$. The positive charges in metal ion-benzocrown complexes are partly delocalized over the benzene ring supporting the further efficient stabilization of negatively-charged SWNTs. In addition to this charge-delocalization effect, we expect a substantial effect of π-π interactions associated with the partially charged benzene ring of benzocrown ethers onto SWNTs, which may further stabilize the n-type SWNTs. The well-known matching rule of crown ether's pocket and cation size (**Figure S11**) also supported this speculation.[29]

3. Conclusion

In summary, SWNTs treated with salts and crown ether exhibited n-type thermoelectric performance with excellent air- and heat-stability even at 150 °C. The efficient and stable n-

type doping of SWNTs involves 1) the moderate reduction of SWNTs induced by electron transfer from the small anions, and 2) the specific stabilization of negatively charged SWNTs. The soft counter cations such as $[M\text{-crown}]^+$ and R_4N^+ are crucial for both effects, which are readily explained in terms of the HSAB rule. The present n-type doping procedure is not limited for SWNTs but also applicable for some other nanocarbons such as multi-walled CNTs and graphenes. These thermally-stable n-type materials may also be applicable for the development of future electronic devices, including n-type or ambipolar FETs (**Figure S12**). The materials showed sufficient stability under a vacuum condition and could be compatible for usual device production processes such as metal deposition with the conventional sputtering procedure, which remains to be explored.

4. Experimental Section

Sample preparation: We used three SWNTs, typically depicted as KH-CNTs (KH Chemicals KH SWCNT HP, >80 wt% carbon content, 1.0-1.4 (1.3) nm in diameter, 5-50 μm in length), Tuball-CNTs (OCSiAl, >75 wt% carbon content, 1.8±0.3 nm in diameter), and eDIPS-CNTs (Meijo Nanocarbon EC2.0, >90 wt% carbon content, 2.0±0.7 nm in diameter). Conducting samples for thermoelectric measurements were prepared by the filtration of sonicated SWNT dispersion (QSONICA Q-125), prior to the doping. Doping was carried out by dipping SWNT films typically in methanol solution of 0.1 mol/L salt and crown ether solution or 0.1 mol/L onium salts.

Characterization: Electrical conductivity was measured using a four-point probe method (Mitsubishi Chemical Analytech Loresta MCP-T610). The through-plane electrical conductivity was evaluated following the literature,[52] and validated using copper, aluminum and SUS304 plates as a reference. The in-plane Seebeck coefficient was recorded using a Seebeck coefficient measurement system (MMR technologies K20SB100-3R) with a Joule–Thomson effect temperature controller. The through-plane Seebeck coefficient was evaluated

by measuring the voltage of samples between hot and cold sides, and their temperature difference was determined using a constantan wire as a reference. Temperature difference was applied using two heat blocks. Work function was evaluated using ultraviolet photoelectron spectroscopy in air (Riken Keiki AC-3). TEM observations were carried out using a JEOL JEM-3100FEF at an acceleration voltage of 300 kV with EDS and EELS analyzer. For TEM, SWNTs was transferred on Cu microgrids (Ohken Shoji STEM 100Cu) by stamping them on the sample. In-plane and through-plane thermal diffusivity was evaluated using a home-built periodic laser heating method reported elsewhere (**Figure S13**),[50] and Xenon flash analyzer (NETZSCH LFA 467), respectively. Heat capacity was measured using differential scanning calorimetry (NETZSCH DSC 204 F1 Phoenix).

Supporting Information
Experimental details for procedures, basic characterization and some application in polymer composites and field effect transistors. Supporting Information is available from the Wiley Online Library or from the author.

Acknowledgements
We acknowledge Sakiko Fujita, Fumio Asanoma, and Yasuo Okajima (NAIST technical staff) for their technical assistance. We thank Mayuko Shido (NETZSCH Japan) for help with the through-plane thermal diffusivity and DSC measurements. We also acknowledge Prof. Leigh McDowell (NAIST) for his careful proofreading of the manuscript. This work was funded by Grant-in-Aid for Young Scientists (B) (Grant no. 26790014) of Japan Society for the Promotion of Science (JSPS KAKENHI), and the Green Photonics Research Project supported by Ministry of Education, Culture, Sports, Science and Technology (MEXT), Japan. This work made use of NAIST common facilities supported by the MEXT Nanotechnology Platform program.

Received: ((will be filled in by the editorial staff))
Revised: ((will be filled in by the editorial staff))
Published online: ((will be filled in by the editorial staff))

[1] A. Javey, J. Guo, Q. Wang, M. Lundstrom, H. Dai, H. *Nature* **2003**, *424*, 654.

[2] M. Campoy-Quiles, T. Ferenczi, T. Agostinelli, P. G. Etchegoin, Y. Kim, T. D. Anthopoulos, P. N. Stavrinou, D. D. C. Bradley, J. Nelson, *Nat. Mater.* **2008**, *7*, 158.

[3] C. Yu, L. Shi, Z. Yao, D. Li, A. Majumdar, *Nano Lett.* **2005**, *5*, 1842.

[4] A. Sekiguchi, F. Tanaka, T. Saito, Y. Kuwahara, S. Sakurai, D. N. Futaba, T. Yamada, K. Hata, *Nano Lett.* **2015**, *15*, 5716.

[5] C. Yu, K. Choi, L. Yin, J. C. Grunlan, *ACS Nano* **2011**, *5*, 7885.

[6] M. Xu, D. N. Futaba, T. Yamada, M. Yumura, K. Hata, *Science* **2010**, *330*, 1364.

[7] T. Takenobu, T. Takano, M. Shiraishi, Y. Murakami, M. Ata, H. Kataura, Y. Achiba, Y. Iwasa, *Nat. Mater.* **2003**, *2*, 683.

[8] S. A. Hodge, S. Fogden, C. A. Howard, N. T. Skipper, M. S. P. Shaffer, *ACS Nano* **2013**, *7*, 1769.

[9] K. Yanagi, S. Kanda, Y. Oshima, Y. Kitamura, H. Kawai, T. Yamamoto, T. Takenobu, Y. Nakai, Y. Maniwa, *Nano Lett.* **2014**, *14*, 6437.

[10] H. Wang, P. Wei, Y. Li, J. Han, H. R. Lee, B. D. Naab, N. Liu, C. Wang, E. Adijanto, B. C.-K. Tee, S. Morishita, Q. Li, Y. Gao, Y. Cui, Z. Bao, *Proc. Natl. Acad. Sci. U.S.A.* **2014**, *111*, 4776.

[11] P. Wei, N. Liu, H. R. Lee, E. Adijanto, L. Ci, B. D. Naab, J. Q. Zhong, J. Park, W. Chen, Y. Cui, Z. Bao, *Nano Lett.* **2013**, *13*, 1890.

[12] W. Chen, L. Duan, D. Zhu, *Environ. Sci. Technol.* **2007**, *41*, 8295.

[13] Y. Chen, J. Chen, H. Hu, M. A. Hamon, M. E. Itkis, R. C. Haddon, *Chem. Phys. Lett.* **1999**, *299*, 532.

[14] R. Saito, M. Hofmann, G. Dresselhaus, A. Jorio, M. S. Dresselhaus, *Adv. in Phys.* **2011**, *60*, 413.

[15] P. Avouris, *Acc. Chem. Res.* **2002**, *35*, 1026.

[16] R. S. Lee, H. J. Kim, J. E. Fischer, A. Thess, R. E. Smalley, *Nature* **1997**, *388*, 255.

[17] O. Chauvet, G. Baumgartner, M. Carrard, W. Bacsa, D. Ugarte, W. A. deHeer, L. Forro, *Phys. Rev. B* **1996**, *53*, 13996.

[18] C. Zhou, J. Kong, E. Yemilmez, H. Dai, *Science* **2000**, *290*, 1552.

[19] B. H. Kim, T. H. Park, T. H. Baek, D. S. Lee, S. J. Park, J. S. Kim, Y. W. Park, *J. Appl. Phys.* **2008**, *103*, 096103.

[20] Z. Li, L. M. Guard, J. Jiang, K. Sakimoto, J. S. Huang, J. Wu, J. Li, L. Yu, R. Pokhrel, G. W. Brudvig, S. Ismail-Beigi, N. Hazari, A. D. Taylor, *Nano Lett.* **2014**, *14*, 3388.

[21] T. Fukumaru, T. Fujigaya, N. Nakashima, *Sci. Rep.* **2015**, *5*, 7951.

[22] M. Shim, A. Javey, N. W. S. Kam, H. Dai, *J. Am. Chem. Soc.* **2001**, *123*, 11512.

[23] S. M. Kim, J. H. Jang, K. K. Kim, H. K. Park, J. J. Bae, W. J. Yu, I. H. Lee, G. Kim, D. D. Loc, U. J. Kim, E.-H. Lee, H.-J. Shin, J.-Y. Choi, Y. H. Lee, *J. Am. Chem. Soc.* **2009**, *131*, 327.

[24] B. D. Naab, S. Guo, S. Olthof, E. G. B. Evans, P. Wei, G. L. Millhauser, A. Kahn, S. Barlow, S. R. Marder, Z. Bao, *J. Am. Chem. Soc.* **2013**, *135*, 15018.

[25] Y. Nonoguchi, K. Ohashi, R. Kanazawa, K. Ashiba, K. Hata, T. Nakagawa, C. Adachi, T. Tanase, T. Kawai, *Sci. Rep.* **2013**, *3*, 3344.

[26] C. Yu, A. Murali, K. Choi, Y. Ryu, *Energy Environ. Sci.* **2012**, *5*, 9481.

[27] C. Wan, X. Gu, F. Dang, T. Itoh, Y. Wang, H. Sasaki, M. Kondo, K. Koga, K. Yabuki, K. J. Snyder, R. Yang, K. Koumoto, *Nat. Mater.* **2015**, 14, 622.

[28] A. R. Siekkinen, J. M. McLellan, J. Chen, Y. Xia, *Chem. Phys. Lett.* **2006**, *432*, 491.

[29] It is worth to note that KF/18-crown ether mixture also forms n-type SWNTs, which is in marked contrast to the previously reported HF treatment inducing oxygen removal from SWNTs. X. Li, J. S. Huang, S. Nejati, L. McMillon, S. Huang, C. O. Osuji, N. Hazari, A. D. Taylor, *Nano Lett.* 2014, *14*, 6179.

[30] G. W. Gokel, D. M. Goli, C. Minganti, L. Echegoyen, *J. Am. Chem. Soc.* **1983**, *105*, 6786.

[31] D. J. Sam, H. E. Simmons, *J. Am. Chem. Soc.* **1974**, *96*, 2252.

[32] *Chemical Abstracts (basic), 5th edition*; (Eds: Chemical Society of Japan), Maruzen, Tokyo **2004**, pp II-579–II-584.

[33] S. E. F. Kleijn, S. C. S. Lai, M. T. M. Koper, P. R. Unwin, *Angew. Chem. Int. Ed.* **2014**, *53*, 3558.

[34] J. C. Byers, A. G. Güell, P. R. Unwin, *J. Am. Chem. Soc.* **2014**, *136*, 11252.

[35] D. T. Sawyer, J. R. Roberts Jr., *Acc. Chem. Res.* **1988**, *21*, 469.

[36] U. Mayer, V. Gutmann, W. Gerger, *Monatshefte ffir Chemie* **1975**, *106*, 1235.

[37] K. Maity, D. K. Panda, E. Lochner, S. Saha, *J. Am. Chem. Soc.* **2015**, *137*, 2812.

[38] M. Shiraishi, M. Ata, *Carbon* **2001**, *39*, 1913.

[39] C. K. Mai, B. Russ, S. Fronk, N. Hu, M. B. Chan-Park, J. J. Urban, R. A. Segalman, M. L. Chabinyc, G. C. Bazan, *Energy Environ. Sci.* **2015**, *8*, 2341.

[40] K.Shi, F. Zhang, C. A. Di, T. W. Yan, Y. Zou, D. Zhu, J. Y. Wang, J. Pei, *J. Am. Chem. Soc.* **2015**, *137*, 6979.

[41] R. M. Ireland,Y. Liu, X. Guo, Y.-T. Cheng, S. Kola, W. Wang, R. Yang, M. L. Falk, T. Jones, H. E. Katz, *Adv. Sci.* **2015**, *2*, 1500015.

[42] O. Bubnova, Z. U. Khan, A. Malti, S. Braun, M. Fahlman, M. Berggren, X. Crispin, *Nat. Mater.* **2011**, *10*, 429.

[43] G. H. Kim, L. Shao, K. Zhang, K. P. Pipe, *Nat. Mater.* **2013**, *12*, 719.

[44] T. Park, C. Park, B. Kim, H. Shin, E. Kim, *Energy Environ. Sci.* **2013**, *6*, 788.

[45] Q. Wei, M. Mukaida, K. Kirihara, Y. Naitoh, T. Ishida, *Appl. Phys. Express* **2014**, *7*, 031601.

[46] N. Toshima, K. Oshima, H. Anno, T. Nishinaka, S. Ichikawa, A. Iwata, Y. Shiraishi. *Adv. Mater.* **2015**, *27*, 2246.

[47] C. Cho, B. Stevens, J.-H. Hsu, R. Bureau, D. A. Hagen, O. Regev, C. Yu, J. C. Grunlan, *Adv. Mater.* **2015**, *27*, 2996.

[48] M. He, J. Ge, Z. Lin, X. Feng, X. Wang, H. Lu, Y. Yang, F. Qiu, *Energy Environ. Sci.*, **2012**, *5*, 8351.

[49] M. He, F. Qiu, Z. Lin, *Energy Environ. Sci.*, **2013**, *6*, 1352.

[50] R. Kato, A. Maesono, R. P. Tye, I. Hatta. *Int. J. Thermophysics* **1999**, *20*, 977.

[51] Doped SWNTs exhibited roughly 2.5 times larger diffusivity with the almost same heat capacity and increased mass density probably because drying-induced zipping and then slight densification of CNT bundles may result in an increase in phonon path. Instead, through-plane conductivity decreased from 0.139 to 0.124 W/mK after n-type doping. This fact further supports our consideration that improved CNT alignment after doping modulates the anisotropic thermal conductivity. As a result, we estimated a 4.4-fold increase in the anisotropy ($k_{//} / k_{\perp}$).

[52] Q. Wei, M. Mukaida, K. Kirihara, T. Ishida, *ACS Macro Lett.* **2014**, *3*, 948.

[53] D. D. Freeman, K. Choi, C. Yu, *PLoS ONE*, **2012**, *7*, e47822.

[54] C. J. DuBois, K. A. Abboud, J. R. Reynolds, *J. Phys. Chem. B* **2014**, *108*, 8550.

Highly stable n-type nanocarbon materials are prepared using the complexes of ordinary salts and crown ethers. Negatively charged π-conjugated structures in n-type materials are stabilized by the coordination of soft acids on the basis of classical *hard and soft acids and bases* (HSAB) theory. The exceptional thermal stability of n-type single-walled carbon nanotubes at 150 °C in air is demonstrated.

doping, stability, redox reactions, coordination, carbon nanotubes

Y. Nonoguchi,* M. Nakano, T. Murayama, H. Hagino, S. Hama, K. Miyazaki, R. Matsubara, M. Nakamura, T. Kawai*

Simple Salt-coordinated n-Type Nanocarbon Materials Stable in Air

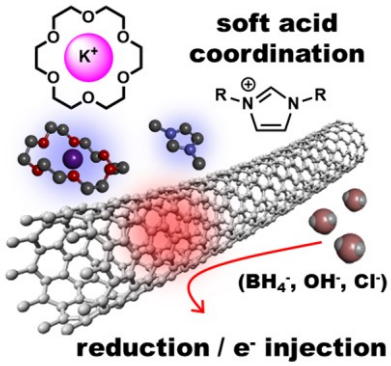

ToC figure (55 mm broad × 50 mm high, 300DPI)